Study of Higher Hydrocarbon Production during Ethylacetylene Pyrolysis Using Laser-Generated Vacuum-Ultraviolet Photoionization Detection

James Boyle and Lisa Pfefferle*

Department of Chemical Engineering, Yale University, New Haven, Connecticut 06520
(Received: November 3, 1989; In Final Form: February 16, 1990)

Higher hydrocarbon formation during the pyrolysis of ethylacetylene in a microjet reactor was studied by vacuum-ultraviolet photoionization time-of-flight mass spectrometry. At the wavelength employed, this ionization technique allows for the simultaneous detection of both stable and intermediate polyatomic species with ionization potentials below 10.49 eV, including most hydrocarbons with two or more carbon atoms. Minimal fragmentation simplifies the determination of parent species and allows identification of probable reaction pathways involving hydrocarbon radicals as well as stable species. The pyrolysis of ethylacetylene was carried out in the fast-flow microjet reactor (residence times 1–2 ms) at temperatures from 300 to 1600 K. At temperatures below 1500 K, products are predominantly linear conjugated compounds that are either primary pyrolysis products such as C_3H_3 or products of C_1 and C_2 addition and abstraction reactions. The first greater than four carbon hydrocarbons to be detected at 2-ms residence time were mass 78, at 1450 K, and mass 92, at 1280 K (likely predominantly benzene and toluene, respectively). At higher reactor temperatures, a progression of polymerization products was observed including likely aromatic species. Accompanying this increase, particularly above temperatures of 1600 K, are dramatic decreases in the concentration of species with fewer than 10 carbon atoms, due to their combination to form large polyaromatic hydrocarbon species. Analysis of the data shows that production rates of masses 78 and 92 amu are consistent with a low activation energy reaction of C_4H_5 with acetylene and methylacetylene (propyne). A mechanism involving the recombination of C_3H_3 radicals followed by isomerization can also account for mass 78 production, assuming it proceeded at a high-pressure-limit recombination rate which has been estimated by previous investigators.

I. Introduction

The purpose of this study is to experimentally investigate the high-temperature decomposition of ethylacetylene and subsequent polymerization to higher hydrocarbons. Specifically, measured production rates for higher hydrocarbon species can provide insight into the mechanisms for formation of soot precursor species. Ethylacetylene was chosen because it was expected to produce C_3H_3, a possible benzene precursor, as a primary decomposition product.

The starting point for all investigations into high-temperature chemical mechanisms leading to higher hydrocarbon and soot formation in flames is the following experimentally observed phenomena. First, large polyaromatic hydrocarbon (PAH) structures obtained from a variety of reaction schemes, under both pyrolytic and oxidative conditions, are chemically identical (e.g., refs 1 and 2), despite the variations of reaction time, temperature, and/or initial chemistry. This strongly suggests a predominant overall mechanism governing soot precursor formation. Second, experiments with different fuels under pyrolytic conditions both in fast-flow reactors and in diffusion flames have shown markedly different propensities to produce these large PAH structures, whose concentrations can be correlated to initial soot production rates.[3] Therefore, under these conditions, individual pyrolysis routes (which are a function of the initial fuel structure) will likely control production of species that take part in the rate-limiting step to soot precursor production.

A detailed mechanism for the formation of ring structures which lead to soot has been proposed by Frenklach and co-workers.[4,5] This mechanism assumes the initial formation of the first aromatic ring (benzene) to be the rate-limiting step for soot formation, and it provides a rationale for the fuel-dependent soot yields observed by previous researchers (e.g., ref 3). Fuel chemistry beyond the two aromatic ring stage was not considered, since similarity between different systems is virtually complete by this step with growth rates being much faster than for the formation of the initial ring structure.

Many other investigators have proposed mechanisms for the formation of benzene and higher hydrocarbons from light hydrocarbon fuels (e.g., refs 1–23). Westmoreland et al.[14] have reviewed these mechanisms and derived a rate of production analysis using bimolecular QRRK calculations to estimate the contribution from various postulated reaction channels in acetylene flames. They concluded that observed production rates for benzene formation can be accounted for through reactions such as

$$C_4H_5 + C_2H_2 \rightarrow C_6H_6 + H \quad (1)$$

or

$$C_4H_3 + C_2H_2 \rightarrow \text{phenyl} \quad (2)$$

(1) Colket, M. B. *Symp. (Int.) Combust., [Proc.], 21st* **1986**, 851.
(2) Lam, F. W.; Howard, J. B.; Longwell, J. *Sym. (Int.) Combust., [Proc.], 22nd* **1988**, 323.
(3) Takahashi, F.; Glassman, I. *Combust. Sci. Technol.* **1984**, *37*, 1.
(4) Frenklach, M.; Clary, D. W.; Gardiner, W. C.; Stein, S. E. *Symp. (Int.) Combust., [Proc.], 20th* **1984**, 887.
(5) Frenklach, M. *Symp. (Int.) Combust., [Proc.], 22nd* **1988**, 1075.
(6) McKinnon, J. T.; Howard, J. B. Presented at the Combustion Institute Eastern States Meeting, Dec 1987.
(7) Bockhorn, H.; Fetting, F.; Wenz, H. W. *Ber. Bunsen-Ges. Phys. Chem.* **1983**, *87*, 1067.
(8) Kern, R. D.; Singh, H. J.; Esslinger, M. A.; Winkeler, P. W. *Symp. (Int.) Combust., [Proc.], 19th* **1982**, 1351.
(9) Olson, K. L.; Harris, S. J.; Weiner, A. M. *Combust. Sci. Technol.* **1987**, *51*, 97.
(10) Bittner, J. D.; Howard, J. B. *Symp. (Int.) Combust., [Proc.], 18th* **1981**, 1105.
(11) Cole, J. A.; Bittner, J. D.; Longwell, J. P.; Howard, J. B. *Combust. Flame* **1984**, *56*, 51.
(12) Glassman, I. *Symp. (Int.) Combust., [Proc.], 22nd* **1989**, 295.
(13) Brezinsky, K.; Hura, H. S.; Glassman, I. *Energy Fuels* **1988**, *2*, 487.
(14) Westmoreland, P. R.; Dean, A. M.; Howard, J. B.; Longwell, J. P. *J. Phys. Chem.* **1989**, *93*, 8171–8180.
(15) Miller, J. H.; Mallard, W. G.; Smith, K. C. *Symp. (Int.) Combust., [Proc.], 21st* **1986**, 1057–1065.
(16) McKinnon, J. T.; Howard, J. B. Critical Testing of Soot Nucleation Mechanisms. Presented at the 19th Biennial Conference on Carbon, June 25–30, 1989, Pennsylvania State University.
(17) Harris, S. J.; Weiner, A. M. *Symp. (Int.) Combust., [Proc.], 22nd* **1988**, 333–342.
(18) Colket, M. B.; Seery, D. J. Presented at the 20th International Symposium on Combustion, Ann Arbor, MI, 1984; Poster Paper 55.
(19) Thomas, S. D.; Westmoreland, P. R. Role of C_3H_3 in Aromatics and Soot Formation. Presented at the American Institute of Chemical Engineers Annual Meeting, San Francisco, CA, Nov 5–10, 1989.
(20) Lazzara, C. P.; Biordi, J. C.; Papp, J. F. *Combust. Flame* **1973**, *21*, 371.
(21) Benson, S. W. *J. Chem. Phys.* **1967**, *46*, 4620–4926.
(22) Benson, S. W.; Haugen, G. R. *J. Phys. Chem.* **1967**, *71*, 1735–1746.
(23) Homann, K. H. *Symp. (Int.) Combust., [Proc.] 20th* **1984**, 857.

0022-3654/90/2094-3336$02.50/0

and that production of the aromatic ring is direct rather than through thermal intermediates due to chemical activation of the initial adduct. The reaction channel

$$C_3H_3 + C_3H_3 \rightarrow C_6H_6 \quad (3)$$

was also found to be consistent with experimentally observed benzene production rates in acetylene flames, if it proceeds at a high-pressure-limit recombination rate. This reaction pathway, however, was not considered as likely due to barriers to cyclization and because multiple H atom shifts would be required. Starting with ethylacetylene as the fuel, our expected (and measured) low conversion concentration of C_4H_5 compared to C_4H_3 was very high, leading us to expect the C_4H_5 reaction channel to play a role in the initial production of benzene in this system. In addition, methylacetylene concentration increases faster than acetylene, so we might expect toluene formation via the reaction

$$C_4H_5 + C_3H_4 \rightarrow C_7H_8 + H \quad (4)$$

to precede benzene formation.

As a rationale for our experimental strategy, we note that obtaining accurate reactant and intermediate concentrations in a complex mixture of neutral molecules, radicals, and ions is both difficult and necessary for discriminating among various proposed reaction pathways. Species of importance in identifying reaction pathways may be labile intermediates present in ppm concentrations. Previous measurements of these reactions have been performed primarily using electron impact mass spectrometry (EIMS). High-energy (70–100-eV) EIMS requires detailed knowledge of fragmentation patterns for each species, and thus is not suitable for analysis of complex mixtures without coupling to a separation technique.

Low-energy EIMS using electrons tuned to the ionization potentials of the species of interest is useful in hydrocarbon chemistry studies (e.g., refs. 10, 11, and 24). However, as has been discussed by numerous investigators (e.g., Rosenstock[25] and Chupka[26,27]) using low-energy EIMS, electron ionization cross sections of small polyatomic molecules are relatively low, while their first derivatives with respect to electron energy are very large. Consequently, the accuracy of the absolute concentration measurement is at best a factor of 2 (according to ref 10) and likely worse. Also, the ability to regulate the exact energy of a given electron source as well as to control the field around such a source may show significant use-dependent variation,[26] compounding the error.

GC/MS (e.g., refs 1 and 2) and LC/MS have allowed both verification of stable species product distributions and development of correlations between PAH species production rates and soot production. These techniques do not allow detection of radicals and other labile species that play an important role in kinetic pathways. Nonetheless, from relative concentration profiles of the stable compounds, some important trends have been observed. Lam et al.,[2] using a fast-flow reactor, noted the thermodynamic stability of acetylene and showed a correlation between the observed aromatic growth and net C_2H_2 disappearance, also shown by Harris and co-workers.[17] Resonantly enhanced multiphoton ionization (REMPI) has been used for *nonsimultaneous* detection of aromatic molecules (e.g., refs 28–33). REMPI has a number of advantages including high sensitivity and the capability to distinguish structural isomers. However, in order to detect all the reaction-generated compounds of interest, one would have to sequentially tune the ionizing radiation to as many wavelengths as there were species and have knowledge of ionization efficiency. For the complex mixtures present in most combustion systems of interest, such as "line-by-line" procedure is impractical. In addition, REMPI is inefficient for ionization larger aromatic molecules because ionization requires either a three-photon resonance scheme or an off-resonance ionization scheme, which both entail low sensitivity.[30] Alternately, use of Rydberg states for the ionization process entails a loss of specificity (the advantage of REMPI), especially at larger molecular weights.

Hydrocarbon ionization using single vacuum-ultraviolet photons was first shown by Lossing and Tanaka[34] in 1956 using a krypton resonance lamp. This work demonstrated that vacuum-UV photoionization of hydrocarbons could be highly efficient and that detectable fragmentation could be either avoided or suppressed far below typical electron impact levels. Gutman and co-workers (ref 35 and references therein) have used resonance lamps as vacuum-UV ionization sources in shock tube kinetics studies. Most recently, vacuum-UV photoionization as been applied to the detection of combustion and pyrolysis products.[36] In addition, a number of other groups are using this technique for hydrocarbon reaction studies, for example, Chen et al.[37] for the study of small hydrocarbon radicals, Schuhle et al.[38] for the detection of photodesorbed TCDD and 7-methylguanine, and most recently Woodin et al.[39] for the detection of hydrocarbon pyrolysis products. A comprehensive review of laser-based techniques for vacuum-UV generation is presented by Vidal.[40]

In this study, vacuum-UV radiation is generated by tripling the UV output of an Nd:YAG pumped dye laser system. Laser-generated vacuum-UV radiation is preferable for a combustion kinetics application because it can be effectively coupled with time-of-flight (TOF) detection which provides greater species sensitivity than a resonance lamp/quadrupole combination, in addition to simultaneous detection. By combining this spectrometer and the microjet reactor, we have obtained data for higher hydrocarbon formation kinetics during the pyrolysis of 1-butyne (ethylacetylene, or EA). This particular combination of a reactor which allows sampling with minimum perturbation of the reacting gas combined with a soft ionization mass identification technique has allowed us to demonstrate the role of hydrocarbon radicals in higher hydrocarbon growth processes and to check proposed mechanisms through radical species production rate data. While this study is directed at examining the kinetics of aromatic formation in the 0–200 amu mass range, pyrolysis products as high as 400–700 amu have been generated and detected at longer residence time conditions in this apparatus.

II. Experimental Apparatus

The microjet reactor source, described in detail in ref 36, is similar to the microjet burner used by Groeger and Fenn.[41] It is a miniature fast-flow reactor coupled directly to a sonic nozzle with a volume of approximately 3.2×10^{-9} m^3. The reactor geometry consists of an alumina multibore thermocouple insulator tube inserted into a larger alumina tube with a sapphire or laser-drilled nozzle (50–200 μm). The inner tube is positioned to leave a 1-mm-long reaction chamber and is sealed by fusing powdered alumina over the joints. Reactants (pure ethylacetylene

(24) Smith, R. D.; Johnson, A. L. *Combust. Flame* **1983**, *51*, 1.
(25) Rosenstock, H. M.; Draxl, K.; Steiner, B. W.; Herron, J. T. Energetics of Gaseous Ions. In *Journal of Physical and Chemical Reference Data*; National Bureau of Standards: Washington, DC, 1977; Vol. 6.
(26) Chupka, W. A. Personal communication.
(27) Chupka, W. A. *J. Chem. Phys.* **1959**, *30*, 191.
(28) Kinsel, G. R.; Segar, K. R.; Johnston, M. V. *Org. Mass Spectrom.* **1987**, *22*, 627.
(29) Tembreull, R.; Lubman, D. M. *Anal. Chem.* **1986**, *58*, 1299.
(30) Hager, J. W.; Wallace, S. C. *Anal. Chem.* **1988**, *60*, 5.
(31) Boyle, J.; Pfefferle, L. D. Presented at the Eastern States Combustion Institute Fall Meeting, Dec 1988; Paper 12.
(32) Grotemeyer J.; Schlag, E. W. *Angew. Chem.* **1988**, *27*, 447.
(33) Chupka, W. A. In *Chemical Spectroscopy and Photochemistry in the Vacuum-Ultraviolet*; Sandorfy, C., Ausloos, P. J., Robin, M. B., Eds.; NATO Advanced Study Institute Series; D. Reidel: Dordrecht, Holland, 1973; Vol. 8, p 433.
(34) Lossing, F. P.; Tanaka, I. *J. Chem. Phys.* **1956**, *25*, 1031–1034.
(35) Slagle, I.; Park, J.; Heaven, M. C.; Gutman, D. *J. Am. Chem. Soc.* **1984**, *106*, 4356.
(36) Boyle, J.; Pfefferle, L. D.; LoBue, J.; Colson, S. *Combust. Sci. Technol.*, in press.
(37) Chen, P.; Colson, S.; Chupka, W. A.; Berson, J. A. *J. Phys. Chem.* **1986**, *90*, 2319.
(38) Schuhle, U.; Pallix, J. B.; Becker, C. H. *J. Am. Chem. Soc.* **1988**, *110*, 2323.
(39) Woodin, R. L.; Meyer, C. F.; Porter, R. F. Abstracts of Papers of the American Chemical Society, 190, 1985.
(40) Vidal, C. R. In *Tunable Lasers*; Mollenauer, L. F., White, L. C., Eds.; Springer-Verlag: Berlin, 1985; p 56.
(41) Groeger, W.; Fenn, J. B. *Rev. Sci. Instrum.* **1988**, *59* (9), 1971.

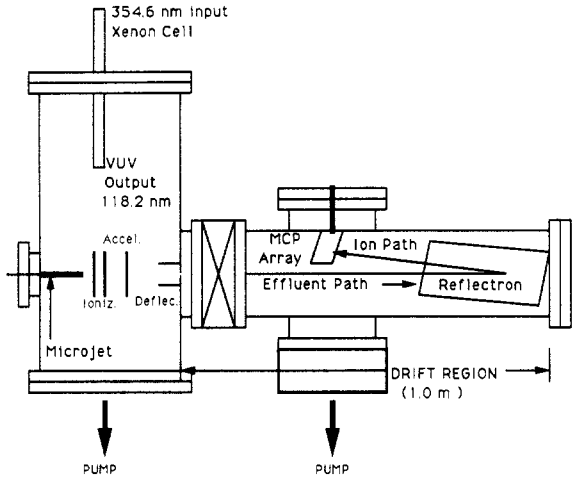

Figure 1. Schematic of the vacuum-ultraviolet time-of-flight mass spectrometer.

in this study) are introduced to the pyrolysis zone through the centermost hole in the inner alumina tube (0.4-mm i.d.) at rates varying from 0.1 to 1.0 sccm. The reaction zone is resistively heated. Temperature within the reactor zone has been calibrated by thermocouples. Thermocouples were not used continuously during experiments due to the catalytic reaction on the platinum/rhodium wires. Pressure within the microjet reactor is monitored upstream by means of a Barotron pressure gauge and was maintained at 400 ± 20 Torr. Under the stated operating conditions, wall reactions do not affect product distributions, and collisions with the wall are much less frequent than molecule–molecule collisions. A test of wall inertness was made through pyrolysis of cyclohexane in both alumina and quartz tubes; this showed no evidence of differences in the mass spectra at temperatures from 300 to 1600 K. While this does not rule out the possibility of catalytic wall effects, the interactions of the high-temperature hydrocarbon intermediates with trace amounts of alkali metals (Na^+ and K^+, detected in focused beams of natural ions from the alumina reactors) were observed to be negligible. Our analysis of this reactor (including modeling of CO/CO_2 production in combustion mode and ion residence time studies) suggests that it can be modeled as a well-mixed reactor. In addition, under the low conversion reaction conditions we use in this study the differential reactor assumption can be used in the analysis of some of the primary reaction channels.

The spectrometer is illustrated in Figure 1. It is equipped with Wiley-McLaren type acceleration for higher resolution and an ion reflectron to compensate for initial ion energy spread, to provide a longer effective flight length (1 m) and to prevent considerable quantities of neutral polymeric hydrocarbons from reaching the detector. Mass signals are displayed in real time and recorded directly onto a digital storage oscilloscope which is interfaced with an IBM PC for data analysis. The mass resolution for the experiments described herein was measured as 325 at 78 amu.

Vacuum-UV photons were generated by the nonlinear optical mixing technique of third-harmonic generation in Xe. A frequency-tripled Nd:YAG laser (Quanta Ray DCR-11 system) operating at 10 Hz was focused into a xenon cell with a 30-cm path length at 26 Torr. The signal from $C_6H_6^+$ produced by single-photon ionization of C_6H_6 from a 300 K fixed flow microjet expansion was used to monitor relative UV to vacuum-UV conversion efficiency. Optimum efficiency was found at approximately 30 mJ of energy in a 8-ns pulse at 354.6 nm, corresponding to a peak power of approximately 3.75×10^6 W. In our experiment the estimated absolute conversion efficiency for vacuum-UV generation using a Xe medium and a DCR-11 laser with a donut beam profile was no greater than 10^{-5}. Slightly higher efficiencies for this particular technique have been reported (ref 41 and references therein) by using either Gaussian beam profiles for the input beam or tuning of the pressure and phase mismatch parameters using mixtures of xenon and other rare gases. Multiphoton processes due to the 354.6-nm light are minimized by using differential focusing.

Ionization efficiencies at 118 nm are relatively constant (±30%) and high for five-carbon hydrocarbons and larger, since these compounds have ionization potentials (IPs) a full 1–2 eV below the photon energy (1182. Å = 10.49 eV). Therefore, the simultaneously obtained peak ratios are assumed good approximations of relative concentration. However, for smaller hydrocarbons with ionization potentials lying closer to the single photon energy, absorption cross sections and ionization efficiencies vary considerably. Consequently, these species must be calibrated individually. We are developing an empirically based correlation based upon available photoelectron spectra and photon yields for a variety of small hydrocarbons[42-45] to obtain more accurate absolute calibration.

Detection efficiencies of the various molecular hydrocarbons must likewise be considered to obtain quantitative data. In the recent work of Geno and MacFarlane,[46] an integrated probability of detection was calculated based upon the relative signals recovered from a variety of small peptides (m/z 86 to m/z 1059). We use this same correlation in our own system, based upon the similarity of hydrocarbons and peptides (hydrocarbons with various attached functional groups). Accordingly, one may then compute a general secondary electron emission coefficient (γ) by

$$\gamma = 2.58 \times 10^{-7} m[\exp(2.31 \times 10^{-4} v)] \quad (5)$$

where m is the molecular weight of the ion (amu) and v is the velocity (m/s). From this value one may then compute the average probability for detecting an ion from the following:

$$P = 1 - e^{-\gamma} \quad (6)$$

Applying these relationships to our own experimental operating conditions (2-kV postacceleration), the average probability of detecting hydrocarbon ions impacting on the microchannel plate is essentially unity through 150 amu. For ions larger than approximately biphenyl, however, corrections must be applied in order to recover relative incident flux at the detector face.

Since only masses are detected, the identity of structural isomers can only be inferred from arguments of internal consistency or knowledge of kinetic constants.

III. Experimental Results and Discussion

1. Initial Pyrolysis of Ethylacetylene. As temperature was increased from 300 to 1270 K at a mean residence times of 2 ms, only the reactant, ethylacetylene, ethylacetylene ± H, methylacetylene (±H), and smaller fragmentation peaks were detected above ppm concentration levels. C_3H_3 was the first pyrolysis product observed, and CH_3 production occurs concurrently with C_3H_3, indicating the initial breakdown of the ethylacetylene occurs via the reaction mechanism

$$C_4H_6 \rightarrow C_3H_3 + CH_3 \quad (7)$$

with a measured activation energy of approximately 60 kcal/mol. The reaction is 34.8 kcal/mol endothermic. At a somewhat higher temperature (1450 K), the major pathway for C_4H_6 destruction is through hydrogen abstraction reaction of C_4H_6 with CH_3 or C_3H_3. The apparent activation energy for C_3H_4 production is observed to be 31 kcal/mol. This can be estimated because initially it is the largest reaction involving methylacetylene, with $[C_3H_4] \gg [C_4H_6]$ and with the thermal decomposition rate of C_3H_4 during this initial period calculated to be a small contributor (<1%). This

(42) Person, J. C.; Nicole, P. P. *J. Chem. Phys.* **1970**, *53*, 1767.
(43) Yoshimo, M.; Takeushi, J.; Suzuki, H. *J. Phys. Soc. Jpn.* **1973**, *34*, 1039.
(44) Parr, A. C.; Elder, F. A. *J. Chem. Phys.* **1968**, *49*, 2659.
(45) Omura, I.; Kaneko, T.; Yamada, Y.; Tanaka, K. *J. Phys. Soc. Jpn.* **1969**, *27*, 178.
(46) Geno, P. W.; MacFarlane, R. D. *Int. J. Mass Spectrom. Ion Processes* **1989**, *92*, 195.
(47) Olson, D. B.; Calcote, H. F. *Symp. (Int.) Combust., [Proc.], 18th* **1981**, 453–464.

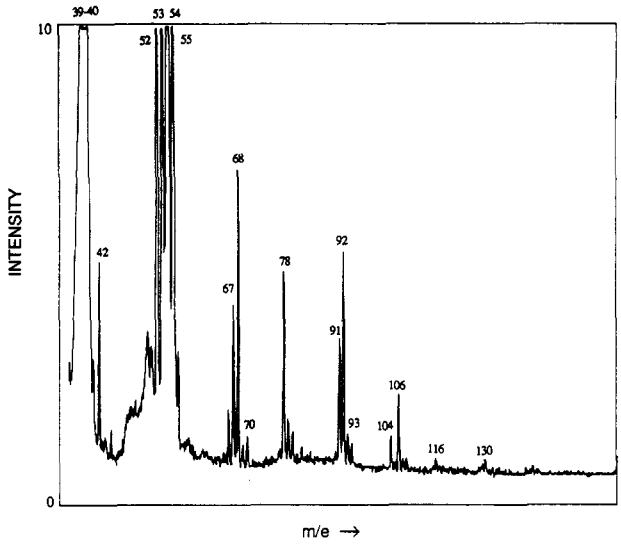

Figure 2. Time-of-flight mass spectra of ethylacetylene pyrolysis products (T = 1530 K, 2-ms reaction time). Intensity is in arbitrary units. The ethylacetylene peak is off-scale.

is higher than the activation energy expected for H atom abstraction by CH_3 of similarly bonded hydrogens in small hydrocarbons, indicating that the reaction of $C_3H_3 + C_4H_6$ to C_3H_4 is fast with respect to the initial pyrolysis step. For a residence time of 2 ms, total conversion of C_4H_6 was on the order of 1% until 1580 K, at which point rapid breakdown occurs as evidenced by a sharp increase in conversion to about 10% by 1620 K.

2. Production of Higher Hydrocarbons. At 1280 K, a series of larger hydrocarbon species are observed just above our lower detection limit, indicating the onset of pyrolysis and subsequent polymerization. More significant polymerization is detected at a temperature of 1450 K at 2 ms. The first compounds with more than four carbon atoms to appear are C_5H_8, C_6H_6, C_7H_8, and C_8H_8. C_7H_8 (likely toluene) is the first higher hydrocarbon to be observed above our detection limits (at 1280 K, 2 ms), followed by C_6H_6 (at 1450 K, 2 ms). Each of these compounds, as well as minor concentrations of other C_5, C_6, C_7, and C_8 species is clearly evident at 1480 K and the same reactor residence time. Conversion of ethylacetylene at this point is approximately 1%.

Figure 2 shows a sample raw TOF mass spectrum for 1530 K and 2-ms reaction time. Groups of products were observed at around mass 92, masses 104 and 106, mass 116, and masses 128–130 and 142–144. As temperature is increased above 1530 K, species are observed at practically every possible molecular weight for an allene or alkyne addition. An interesting observation is that until 1530 K species detected contain a component of linear conjugated structures as predicted from formation mechanisms for the higher molecular weight products observed, such as 106 amu (observed at 1480 K) and 144 amu (observed at temperatures as low as 1530 K). The stoichiometry of these compounds, with relatively high hydrogen content, suggests their formation from smaller noncyclic compounds.

Among the C_5 compounds, for 2-ms reaction time, mass 68 (C_6H_8, likely pentadiene isomers) is apparent at lower temperatures (1450 K) than masses 66 (C_5H_6, likely pentadienyne isomers, at 1510 K) and 67 (1480 K). Mass 68 is likely formed through

$$C_4H_6 + CH_3 \rightarrow C_5H_9 \rightarrow \text{fast } C_5H_8 \qquad (8)$$

The reaction

$$C_4H_5 + CH_4 \rightarrow C_5H_9 \rightarrow \text{fast } C_5H_8 \qquad (9)$$

is endothermic by 6 kcal/mol and thus would likely have a large forward activation energy which was not observed. An apparent activation energy of 20 ± 6 kcal/mol was observed for C_5H_8 production normalized to ethylacetylene and estimated methyl radical concentrations. Masses 66 and 67 could be formed through the following reaction mechanism:

$$C_4H_4 + CH_3 \rightarrow C_5H_7 \rightarrow \text{slow } C_5H_6 \qquad (10)$$

TABLE I: Relative Concentrations of C_5 and Larger Species from the Pyrolysis of Ethylacetylene at 2-ms Residence Time

	temperature, K						
mol wt	1480	1510	1530	1545	1580	1620	1660
66	*b*	3.9	15.3	27.5	49.0	229.7	110.0
67	11.3	16.3	46.0	64.4	93.0	200.0	61.0
68	25.0	37.7	86.0	108.0	122.0	440.0	110.0
78	17.5	26.3	56.0	81.6	112.0	450.0	118.0
79	3.5	7.8	12.8	17.6	24.0	52.8	49.0
80	3.1	4.6	8.8	14.0	29.5	54.0	52.0
91	16.0	22.8	37.0	45.0	56.5	72.5	42.0
92	23.0	36.4	80.0	110.0	144.0	380.0	140.0
93	3.5	7.8	9.0	12.0	15.0	24.0	16.5
94	*b*	4.7	6.8	8.5	11.9	23.8	12.0
104	2.0	3.6	9.5	17.4	29.0	82.5	84.5
106	7.5	13.4	22.0	34.5	42.0	82.5	46.0
116	*a*	*a*	3.2	4.8	12.8	40.0	40.0
118	*a*	*a*	*a*	3.0	7.5	18.0	19.5
128	*a*	*a*	*b*	*b*	7.0	20.0	29.0
130	*a*	*a*	3.2	8.0	16.0	40.0	33.5
142	*a*	*a*	*b*	3.2	4.8	17.6	38.5
144	*a*	*a*	*b*	4.8	6.4	16.8	21.0
102				*a*	*b*	8.5	17.0
152				*a*	*a*	*a*	7.8
154				*a*	*b*	6.0	15.5
156				*a*	*b*	6.0	12.4
166				*a*	*b*	4.5	10.8
168				*a*	*b*	4.5	8.0
170				*a*	*b*	3.0	3.0
178				*a*	*a*	*a*	5.4
180				*a*	*a*	*a*	7.0
182				*a*	*a*	*a*	3.0
192				*a*	*a*	*a*	4.5

[a] Species present in 0–1 unit. [b] Species present in 1–2 units. 1 unit is equivalent to 2–5 ppm.

An Arrhenius plot for C_5H_6 formation from C_4H_7 yields a straight line with an apparent activation energy of approximately 30 kcal/mol. An Arrhenius plot for the initial formation of C_5H_7 formation normalized to relative C_4H_4 yields an activation energy of approximately 35 kcal/mol; however, multiple disappearance and production mechanisms are apparent at 1545 K. Mass 67 (C_5H_7) is a relatively stable radical. For 2-ms reaction time, the concentration of mass 67 is greater than that of mass 66 until 1580 K.

3. Cyclic Compound Formation and Competitive Growth at Higher Temperatures. Table I shows relative concentrations of all compounds detected as a function of temperature at 2-ms reaction time. Species indicated by *a* and *b* were detected in concentrations less than 2 units, where 1 unit corresponds to 2–5 ppm.

As temperature is increased, evidence for multiple ring cyclic compounds is observed. An indication of a shift to cyclic structures is the shift in the overall C/H ratio, indicating that highly unsaturated structures dominate as temperature is increased from 1450 to 1620 K. Over this range, there is an exponential increase in the ratios of masses 104/106 and 142/144. In a study of benzene pyrolysis, Smith and Johnson[24] showed that the predominant hydrocarbon products with more than six carbon atoms formed in this temperature and pressure range were C_8H_6 (amu 102), $C_{10}H_8$ (amu 128), $C_{12}H_{10}$ (amu 130), and $C_{12}H_8$ (amu 152). These species are only present in detectable quantities as temperature is increased above 1580 K. Further evidence of cyclic structures appears in the preferential growth at these higher temperatures of species that have been shown to exist in benzene diffusion flames[48] and butadiyne pyrolysis reactions,[23,49] namely, $C_{10}H_8$ (naphthalene), $C_{11}H_{10}$ (methylnaphthalene), and $C_{13}H_{10}$ (methylacenaphthalene).

Mass 78 (C_6H_6) is first detected at 1450 K and is inferred to be primarily benzene from the prominent signals concurrently

(48) Homann, K. H.; Pidoll, U. V. *Ber. Bunsen-Ges. Phys. Chem.* **1986**, *90*, 847.
(49) Wu, C. H.; Kern, R. D. *J. Phys. Chem.* **1987**, *91*, 6291.

detected for 128 amu (likely naphthalene) and 142 amu (likely methylnaphthalene). If we consider benzene formation through the overall mechanism

$$C_4H_5 + C_2H_2 \rightarrow C_6H_7 \rightarrow C_6H_6 + H \quad (1)$$

we can normalize the benzene production rate by the directly measured relative C_4H_5 concentration and the estimated relative C_2H_2 concentration and construct an Arrhenius plot. This plot yields an activation energy of 5 ± 5 kcal/mol (error bars are large because of uncertainty in C_2H_2 estimate), which is consistent with the activation energy reported by Cole et al.[11] Formation of C_6H_6 through the reaction

$$C_3H_3 + C_3H_3 \rightarrow C_6H_6 \quad (3)$$

cannot be ruled out. An estimation of the contribution of this reaction using our measured C_3H_3 concentration and the rate constant reported by other researchers[23,49] yields C_6H_6 concentrations on the same order of magnitude as our observed value, which is within error tolerances for both the measurement and the rate constant uncertainty. In addition, Thomas and Westmoreland[19] recently reevaluated the C_3H_3 pathway to benzene formation in flames in light of the data of Hopf,[50] showing that 1,2,4,5-hexatraene forms benzene and other products at temperatures as low as 500 K. Evidence in favor of reaction 1 as the predominant route to benzene was obtained in our preliminary studies of methylacetylene and allene pyrolysis in the same reactor geometry: allene produced significantly higher concentrations of mass 78 at a given temperature than methylacetylene. This would not be expected if C_3H_3 recombination and isomerization was the predominant route to benzene production because initial pyrolysis rates and C_3H_3 production rates for these isomers are likely similar.[49]

We considered other reaction channels to benzene, including reaction 2. This route through C_4H_3 was considered less likely as the primary route for benzene formation at low ethylacetylene conversions in our system for two reasons. First, benzene production rates rise before the concentration of C_4H_3 reaches significant levels. Second, phenyl radical was not detected in significant quantities. This is inconsistent with a production rate analysis assuming that phenyl radical formation is the main contributor to the measured benzene production rate (based on the estimate of a steady-state concentration of phenyl of at least 50 ppm at 1580 K, which is above our detection limits).

For our reaction conditions (1–4 ms), growth of mass 92 (likely toluene) occurs at a lower temperature than C_6H_6. This is consistent with the overall mechanism

$$C_4H_5 + C_3H_4 \rightarrow C_7H_8 + H \quad (5)$$

because C_3H_4 concentration rises to high levels before acetylene (because it is formed quickly from C_3H_3, which is a primary pyrolysis product of ethylacetylene). An Arrhenius plot of data for the rate of production of mass 92 normalized by the measured relative C_3H_4 and C_4H_5 concentrations yields an activation energy of 4 ± 3 kcal/mol. Other tested routes for mass 92 production resulted in rates significantly below that observed experimentally.

As temperature is increased above 1620 K and reaction time is held constant at 2 ms, signals from species with molecular weights of 110 amu or less level off or decline, and an increasing amount of the total ion current is carried by the C_9 and larger species. This is reflected in product concentrations reported in Table I. Even though ethylacetylene conversion at this temperature and residence time is significant, the total carbon balance on all detected species with fewer than 10 carbon atoms is less at 1660 K than at 1620 K. This is due to the considerable increase in the total ion current for the "high mass" component (C_{10} and larger species). The total ion current of all high mass products as a percent of all products of molecular weight greater than ethylacetylene shifts from 6.8% at 1620 K to 22.9% at 1660 K, indicating the accelerated growth of PAH species.

As temperature and/or residence time are increased above 1620 K and 2 ms, growth of midsize PAH species can be followed quantitatively, including their aryl radical counterparts. This data is interesting as it has become apparent[3,16,17] that reaction/coagulation of PAH species may play an important role in soot nucleation contributing to the consumption of small PAH but not adding to overall soot mass growth. Our data supports this premise: the largest masses observed are formed through combination of other large aromatic hydrocarbon compounds and not by successive addition of acetyl radicals as evidenced by distinct groupings of masses. Other investigators have observed the marked decrease in small PAH at temperatures between 1600 and 1750 K. In a recent paper McKinnon and Howard[16] suggest that the rapid destruction of PAH observed would require a highly activated (ca. 75 kcal/mol) unimolecular pyrolytic process, which is unlikely from analysis of the current data base. Product profiles do not show evidence for a highly activated unimolecular pyrolysis of PAH species which would allow for their rapid consumption at high temperatures.

IV. Conclusion

A microjet reactor coupled to vacuum-UV photoionization was used to study the formation of higher hydrocarbons during the pyrolysis of ethylacetylene. By use of this technique, a progression of intermediate species profiles including hydrocarbon radicals were obtained as a function of temperature. The first pyrolysis product observed was C_3H_3 followed by ethylacetylene ± hydrogen. Subsequent decomposition of C_3H_6 occurred rapidly through H atom abstraction by CH_3 and C_3H_3 to form CH_4 and C_3H_4. Analysis of the measured production rate for the initial cyclic compound detected, toluene, is consistent with formation through $C_4H_5 + C_3H_4$. The production rate for mass 78 (predominantly benzene) is consistent with either a low activation energy reaction of C_4H_5 with acetylene or benzene formation through a multistep reaction involving C_3H_3 recombination followed by isomerization. Consequently, we are currently studying both methylacetylene and allene pyrolysis, both of which are postulated[4] as being precursors of the C_3H_3 radical so that we can differentiate between the two routes for benzene formation. Ethylacetylene was not the optimal choice in discriminating between the two mechanisms because C_3H_3 and C_4H_5 concentrations increased almost concurrently. At temperatures above 1620 K, the concentration of species with nine or more carbons increases dramatically as a significant portion of the detectable carbon appears at increasingly larger masses. This behavior is attributed to addition reactions of larger structures and not by successive addition of acetyl radicals to form linear compounds. These larger structures are believed to be aromatic as evidenced by the predominance of periodic masses throughout the pyrolysis spectra of 0–220 amu.

As noted by Brezinsky et al.,[13] the role of molecular oxygen, especially on reaction channels for initial pyrolysis steps, dictates a certain degree of caution in drawing comparisons between the proposed mechanism of Westmoreland et al. for rich flames and the ethylacetylene pyrolysis data presented here. Consequently, our future work includes examining the impact of oxygen addition on the mechanisms for ethylacetylene, methylacetylene, and allene pyrolysis and combustion using the microjet and vacuum-UV-TOF-MS apparatus. Studies are also under way to investigate the influence of the C_5 compounds (the concentrations of which may be large enough relative to the net production rate of benzene to contribute to aromatic production) using cyclopentadiene. This will allow independent measurement and comparison of cyclopentadiene influence on aromatic growth.

Acknowledgment. We gratefully acknowledge the many helpful discussions with J. B. Fenn and W. A. Chupka. S. Colson, E. E. Gulcicek, and G. Bermudez are thanked for their technical advice. Special thanks to P. Westmoreland (U. Mass.) for discussions concerning reaction mechanisms. We thank NSF grants CBT-8657648 and CBT-8806843 for partial financial support of this work.

Registry No. $H_3CCH_2{\equiv}CH$, 107-00-6.

(50) Hopf, H. *Chem. Ber.* **1971**, *104*, 1499.